Joint Dependence of Longwave Feedback on Surface Temperature and Relative Humidity

Brett McKim[1], Nadir Jeevanjee[2], and Geoffrey K Vallis[1]

[1]University of Exeter
[2]Geophysical Fluid Dynamics Laboratory

November 22, 2022

Abstract

Understanding how the outgoing long-wave radiation (OLR) depends on surface temperature is a climate problem of long standing. Various studies have suggested that clear-sky OLR varies linearly with surface temperature, with a longwave clear-sky feedback that is independent of surface temperature and relative humidity. However, this uniformity lies in tension with the notion that humidity controls tropical stability (e.g. the “furnace” and “radiator fins” of Pierrehumbert, 1995). Here we explore the state-dependence of longwave clear-sky feedback as a function of both surface temperature and column relative humidity. We find that a strong relative humidity-dependence in the feedback emerges above 275 K, stemming from the closing of the H2O window. We construct a simple model for estimating the all-sky feedback and find that although clouds lower the zonal-mean longwave feedback, the dependence on humidity remains significant.

Joint Dependence of Longwave Feedback on Surface Temperature and Relative Humidity

Brett McKim[1], Nadir Jeevanjee[2], Geoffrey K. Vallis[1]

[1]University of Exeter, Exeter, UK
[2]Geophysical Fluid Dynamics Laboratory, Princeton NJ

Key Points:

- The longwave clear-sky feedback exhibits a significant RH-dependence at high temperatures.
- Tropical variations in longwave clear-sky feedback (e.g. "radiator fins") are a consequence of this RH-dependence.
- Cloud radiative effects estimated from a simple model do not qualitatively change this picture.

Corresponding author: Brett McKim, bam218@exeter.ac.uk

Abstract

Understanding how the outgoing long-wave radiation (OLR) depends on surface temperature is a climate problem of long standing. Various studies have suggested that clear-sky OLR varies linearly with surface temperature, with a longwave clear-sky feedback that is independent of surface temperature and relative humidity. However, this uniformity lies in tension with the notion that humidity controls tropical stability (e.g. the "furnace" and "radiator fins" of Pierrehumbert (1995)). Here we explore the state-dependence of longwave clear-sky feedback as a function of both surface temperature and column relative humidity. We find that a strong relative humidity-dependence in the feedback emerges above 275 K, stemming from the closing of the H_2O window. We construct a simple model for estimating the all-sky feedback and find that although clouds lower the zonal-mean longwave feedback, the dependence on humidity remains significant.

Plain Language Summary

The dependence of outgoing longwave radiation radiation (OLR) on surface temperature (i.e. the feedback) is a major determinant of the climate's stability. Various investigators have suggested that the feedback is largely independent of both surface temperature and relative humidity, which implies that the climate stability is also independent of surface temperature and relative humidity. However, this uniformity seems to contradict other work which shows that the subtropics are relatively stable and the deep tropics are relatively unstable, implying the feedback must vary between the two regions. We resolve this apparent contradiction by systematically computing the feedback as a function of both surface temperature and relative humidity. Above 275 K, the feedback depends significantly on relative humidity. We then show the feedback does indeed vary in the tropics and that this difference arises from regional differences in relative humidity. Finally, we estimate the effects of clouds on the feedback with a simple model and find that although clouds have a destabilizing influence, the significant dependence on relative humidity is retained. Our work gives a renewed appreciation for how the feedback can vary significantly with both surface temperature and relative humidity.

1 Introduction

The longwave clear-sky feedback parameter λ_{cs} relates a change in clear-sky outgoing longwave radiation OLR_{cs} to a change in surface temperature T_s,

$$\lambda_{cs} \equiv \frac{\mathrm{dOLR}_{cs}}{\mathrm{d}T_s} \quad (\mathrm{Wm^{-2}K^{-1}}). \tag{1}$$

It is a measure of the stability of the the climate and thus is a well studied quantity, with a canonical value for its global mean of about $2.2\pm10\%$ $\mathrm{Wm^{-2}K^{-1}}$ (Budyko, 1969; R. D. Cess et al., 1989, 1990; Raval et al., 1994; Bony et al., 1995; Allan et al., 1999; Dessler et al., 2008; Chung et al., 2010; Jeevanjee, 2018; Koll & Cronin, 2018; Zhang et al., 2020).

The convergence of the global mean value of λ_{cs} across both observations and the model hierarchy suggests robust physics that is insensitive to the idiosyncrasies of the individual studies. Recently, Koll and Cronin (2018) gave an explanation of this physics as a balance between increasing surface Planck feedback and decreasing surface transmissivity. They verified that $\lambda_{cs} \approx 2.2$ $\mathrm{Wm^{-1}K^{-1}}$ for a wide of T_s in a column model. Zhang et al. (2020) then extended this analysis to GCMs and similarly found λ_{cs} to be independent of both T_s and free-tropospheric relative humidity (RH).

This work on the uniformity of feedback lies in tension with the notion that meridional variations in clear-sky relative humidity are important in controlling tropical stability. In particular, Pierrehumbert (1995) argued that the warm and moist deep tropics, with active deep convection (furnace) are close to a local runaway greenhouse, but are radiatively stabilized by the warm, yet dryer, and more quiescent subtropics (radiator fins). However, Pierrehumbert (1995) was equivocal on whether the furnace and radiator fins manifest as tropical variations in OLR_{cs}, or rather in λ_{cs}, which is the more relevant parameter for stability. Indeed, as we shall show later, the latitudinal variations in OLR_{cs} in the tropics are quite muted compared to OLR_{cs} variations over the globe. Here, then, we will pursue the idea that radiator fins manifest instead as tropical variations in λ_{cs}.

Clouds are another process that may play a role in controlling the structure of zonal-mean feedback. Pierrehumbert (1995) argued for the presence of tropical furnaces and radiator fins using only clear-sky physics. However, humid regions and cloudy regions often go hand-in-hand, and high clouds are known to have a robust influence on the longwave feedback (Zelinka & Hartmann, 2010), so we might expect the longwave all-sky feedback parameter λ_{as} to look different from λ_{cs} in the zonal mean.

We lack clarity on whether the phenomenology of the furnace and radiator fins are better described by OLR_{cs} or by λ_{cs}. Relatedly there is a tension between the constancy of λ_{cs} observed across studies and the notion that humidity variations control tropical stability, and it is unclear how clouds might modulate this relationship. This state of affairs motivates us to ask the following questions:

1. Do furnaces and radiator fins indeed manifest as a contrast in the zonal-mean λ_{cs}?
2. How do we reconcile variations in λ_{cs} implied by furnaces and radiator fins when other studies suggest λ_{cs} is approximately constant?
3. How do clouds modify the meridional structure of longwave feedback?

To this end we first construct a "phase space", in which λ_{cs} is computed as a joint function of T_s and column RH. Below 275 K, we find that λ_{cs} stays within 10% of 2.2 $\mathrm{Wm^{-2}K^{-1}}$, even as RH varies. Above 275 K, however, a significant RH-dependence emerges, leading to much greater variations in λ_{cs}. We show that this RH-dependence stems from the closing of the H_2O window. The tropical contrast in zonal-mean λ_{cs} is, then, a consequence of this RH-dependence at high temperatures. Finally, we construct a simple model for evaluating the all-sky feedback and find that although clouds decrease the zonal-mean feedback, the RH-dependence remains significant.

2 Results

2.1 Exploring the state dependence of λ_{cs}

We first address Question 2, by exploring the state dependence of λ_{cs} as a function of both T_s and RH. We use RH as a state variable because RH-based feedbacks have certain advantages over specific humidity (q_v) based feedbacks both from a thermodynamic point of view (Held & Shell, 2012) and from a radiative point of view (Jeevanjee et al., 2021), as specific humidity already has a de facto strong temperature dependence through the Clausius-Clapeyron relation. To compute radiative transfer we use PyRADS, a validated line-by-line column model (Koll & Cronin, 2019). We used the model in 1-D radiative-convective equilibrium, following (Koll & Cronin, 2018), in which a moist adiabat profile is assumed. We set the CO_2 concentration to 340 ppmv, the number of pressure levels to 30, and consider a spectral range between 0.1 and 3500 $\mathrm{cm^{-1}}$ at 0.01 $\mathrm{cm^{-1}}$ resolution. We only then need to specify the surface temperature and a vertically-uniform relative humidity to compute OLR_{cs} for the column. For more details of atmospheric structure and spectral databases, see "Materials and Methods" in Koll and Cronin (2018).

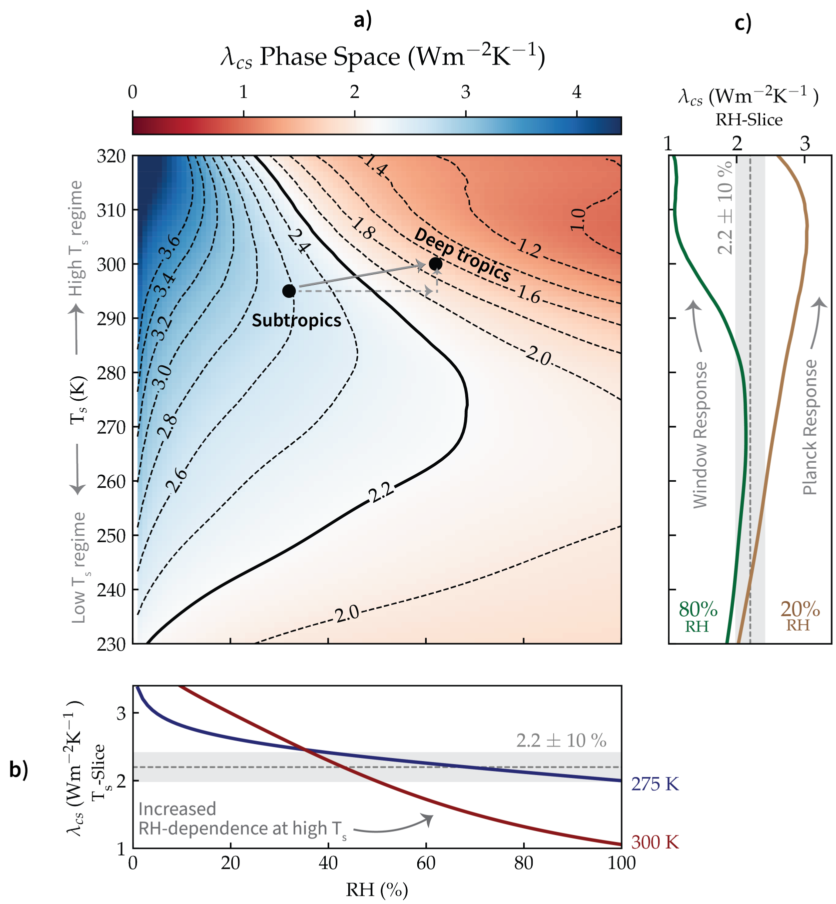

Figure 1. Exploration of state dependence of longwave clear-sky feedback λ_{cs} in a column model. (a) λ_{cs} phase space as a function of surface temperature T_s and column relative humidity RH, with contours indicating values of λ_{cs}. See Equation (2) for details of the calculation. Typical temperatures and humidity of the subtropics and deep tropics are noted as $\sim$295 K/30%, and $\sim$300 K/60%, respectively. The gray arrows indicate different pathways to move from the subtropics to the deep tropics. (b) Cross section of λ_{cs} phase space at 275 K and 300 K. (c) Cross section of λ_{cs} phase space at 20% and 80% relative humidity.

We calculate λ_{cs} in the following way. We first compute OLR_{cs} for some T_s and RH; we then perturb the surface temperature by an amount ΔT, and allow the moist-adiabatic atmosphere to respond while holding RH fixed; finally we calculate the perturbed outgoing longwave radiation and take the finite difference between the two states. In summary:

$$\lambda_{cs} \approx \frac{\text{OLR}_{cs}(T_s + \Delta T, \text{RH}) - \text{OLR}_{cs}(T_s, \text{RH})}{\Delta T}, \tag{2}$$

where $\Delta T = 1$ K in our calculations. Note that the Planck feedback and the lapse-rate feedback are included in λ_{cs}. The moist adiabat is not satisfied in the mid-latitudes, but we note that the lapse-rate feedback is small when RH is fixed (R. Cess, 1975; Held & Shell, 2012; Zelinka et al., 2020; Jeevanjee et al., 2021). We exclude the RH-feedback for simplicity and because its value in the global mean is < 0.1 Wm^{-2}K^{-1} (Held & Shell, 2012; Zelinka et al., 2020).

Our results are summarized in Figure 1a) for surface temperatures between 230 K and 320 K and relative humidities between 0% and 100%. We identify 275 K as the de facto boundary between a low temperature regime and a high temperature regime because each region exhibits distinct behaviors for λ_{cs}. Below 275 K, there is a very small RH-dependence — for values of RH between 20% and 80%, λ_{cs} remains within 10% of 2.2 Wm^{-2}K^{-1}. Above 275 K, however, a significant RH-dependence emerges: the value of λ_{cs} differs from 2.2 Wm^{-2}K^{-1} $\pm$ by much more than 10% over the same range of humidity. We explicitly plot the RH-dependence of λ_{cs} at 275K and 300K (Figure 1b) to highlight this difference in behaviour. Thus, in response to Question 2, a λ_{cs} value of 2.2 Wm^{-2}K^{-1} will occur over much of the globe, and in particular will manifest as the slope of an OLR_{cs} vs T_s regression, as in Figure 1 of Koll and Cronin (2018). Nonetheless, Figure 1 shows that λ_{cs} can still vary considerably at the higher temperatures of Earth's tropics.

2.2 Importance of the H_2O window

This section provides additional context about λ_{cs} by focusing on the underlying radiation physics that controls the climate response.

Since λ_{cs} is dominated by surface emission through the H_2O window (Koll & Cronin, 2018), the wavenumbers at which H_2O absorption is negligible for surface emission, we expect the window to play an important role in the RH-dependence of λ_{cs} at high temperatures. To display the H_2O window, we plot the surface-to-space transmission $\mathcal{T}_\nu$, which measures the portion of surface emission at wavenumber ν that escapes to space. At a surface temperature of 275 K (Figure 2a), the H_2O window remains open as the relative humidity is increased from 12.5% to 100%. At a surface temperature of 300 K (Figure 2b), however, the H_2O window closes rapidly as the relative humidity is increased from 12.5% to 100%. This is due to activation of H_2O continuum absorption (Koll & Cronin, 2018). Thus relative humidity variations are sufficient to close the H_2O window, but only at high temperatures.

Koll and Cronin (2018) emphasized the robustness of $\lambda_{cs} \approx 2.2$ Wm^{-2}K^{-1} as arising from a balance between the closing of the H_2O window and the nonlinear $4\sigma T_s^3$ surface Planck feedback. However, at high temperatures this balance is not guaranteed and depends on RH. The H_2O window closes much faster with temperature at 80% RH than at 20% RH (Figure 2), leading to a "Planck-dominated" response at low RH, and a "window-dominated" response at high RH (Figure 1c).

2.3 Tropical variations in λ_{cs}

In Question 1 we asked whether the furnaces and radiator fins described in Pierrehumbert (1995) manifest as a contrast in the zonal-mean λ_{cs}. To answer this question we will compute time- and zonal-mean T_s and RH from ERA5 reanalysis (Hersbach et al., 2020) and

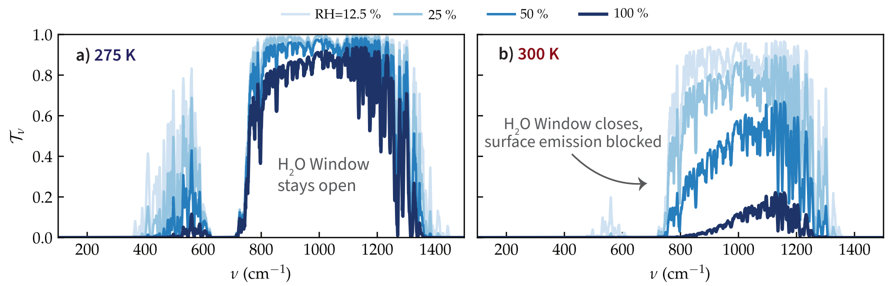

Figure 2. The closing of the H_2O window is sensitive to relative humidity at high surface temperatures. The surface-to-space transmission $\mathcal{T}_\nu$ is plotted as a function of wavenumber ν for a surface temperature of 275 K (a) and 300 K (b), and a relative humidity of 12.5%, 25%, 50%, and 100%. The H_2O window is where $\mathcal{T}_\nu \approx 1$ and surface emission escapes directly to space. We use a SavitzkyGolay filter with a 5 cm^{-1} width to smooth these plots.

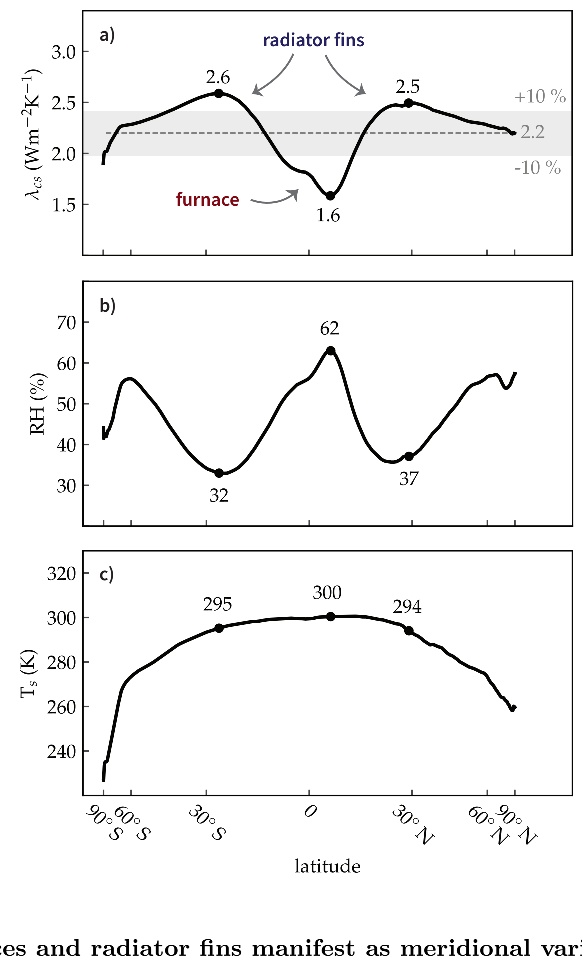

Figure 3. Furnaces and radiator fins manifest as meridional variations in longwave clear-sky feedback λ_{cs}. (a) Zonal-mean λ_{cs} is diagnosed from Figure 1, using the reanalysis zonal-mean RH (b) and the reanalysis zonal-mean T_s (c) as inputs. The shaded region in (a) represents the global mean value of 2.2 $\pm$ 10% Wm^{-2}K^{-1} reported in other studies. We posit that the local maxima and minimum of λ_{cs} that lie outside this range should be considered the "radiator fins" and "furnace", respectively, of the the tropics. Note the equal-area scaling of the x-axis.

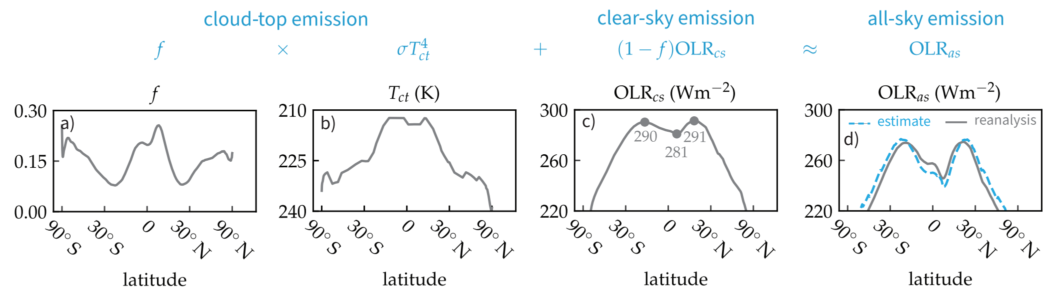

Figure 4. A simple model for zonal-mean all-sky emission. (a) cloud-top fraction f, (b) cloud-top temperature T_{ct}, (c) clear-sky emission OLR_{cs}, and (d) all-sky emission OLR_{as}. The gray curves are from ERA5 reanalyis. The dashed-blue curve in (d) is our simple estimate produced by the equation above the panels (see Equation 3). Note the equal-area scaling of the x-axis.

use these values to read off zonal-mean λ_{cs} from the phase space of Figure 1. We take hourly data sub-sampled every 6 hours from January 1 - December 31, 1981 and compute annual averages. Following Zhang et al. (2020), we calculate a free-tropospheric column RH as the water vapor mass between 850 hPa and the 300 hPa divided by the saturated water vapor mass within the column. Finally, we exclude the boundary layer RH and stratospheric water vapor because of their limited impact on the OLR (Zhang et al., 2020).

We might expect a significant drop in λ_{cs} from the subtropics to the deep tropics by looking at representative values of T_s and RH in the λ_{cs}-phase space (Figure 1). Indeed, the meridional structure of zonal-mean λ_{cs} calculated as described above, shows λ_{cs} varying varies from 2.6 to 1.6 $\text{Wm}^{-2}\text{K}^{-1}$ in the tropics, a 38% drop (Figure 3a). Both the subtropical maxima and deep tropical minimum lie outside the 2.2±10% $\text{Wm}^{-2}\text{K}^{-1}$ range. We posit that these extrema of λ_{cs} should be considered the true "radiator fins" and "furnace", respectively, of the the tropics.

We can test whether the significant drop in λ_{cs} between the radiator fins and the furnace is due to the difference in humidity, as emphasized by Pierrehumbert (1995), or if the drop is due to the difference in temperature. If we look again at the phase space in Figure 1, we can take a path that goes from the subtropics to the deep tropics in two parts: a first part with constant surface temperature, and a second part with constant relative humidity (see the dashed gray arrows). In this region of phase space, the doubling of relative humidity from 30% to 60% causes a much larger change in λ_{cs} than the increase in surface temperature from 295 K to 300 K does.

Our answer to Question 2 is then: zonal-mean λ_{cs} exhibits local extrema, which may be usefully viewed as the furnace and radiator fins of the tropics. Furthermore, these extrema are indeed due to RH variations, consistent with Pierrehumbert (1995). λ_{cs} exhibits a local maxima in the subtropics because they are hot and dry enough for the feedback to exhibit a Planck-dominated response, and λ_{cs} exhibits a local minimum in the deep tropics because it is hot and moist enough for the feedback to exhibit a window-dominated response (Figure 1c).

2.4 Incorporating the effects of cloudiness

In Question 3, we asked whether clouds affect the meridional structure in zonal-mean longwave feedback in the tropics. Rather than explicitly compute cloud feedbacks, which is beyond the scope of this paper, we try to estimate them by constructing a simple model for how clouds modify longwave emission. To validate the approach, we first estimate the all-sky OLR, OLR_{as}, from a few inputs: OLR_{cs}, the cloud-top fraction f, and the cloud-top temperature, T_{ct}. OLR_{cs} is taken directly from ERA5 reanalysis. f is diagnosed from ERA5 reanalysis as the local max of the zonal-mean cloud fraction profile above a 550 hPa threshold, which is used to avoid misidentifying cloud tops with boundary layer cloudiness. T_{ct} is the atmospheric temperature at which cloud fraction profile peaks. We smooth the T_{ct} with a Savitzky-Golay filter with a 10° latitude width to account for sharp jumps in T_{ct} arising from the limited vertical resolution. This method of identifying cloud tops is similar to Thompson et al. (2017). We show our methodology in the SI.

To estimate OLR_{as}, we first consider the effect of high clouds, which block longwave emission from lower levels and replace it with their own longwave emission from cloud tops. We assume high cloud emission acts like a black body and occurs high enough in the atmosphere that emission travels directly to space (Siebesma et al., 2020). As for low clouds, we grossly assume the low clouds emit at a temperature close enough to T_s that they only negligibly alter the outgoing radiation (D. Hartmann, 2015). Given these assumptions, we can now write down a simple expression for OLR_{as}:

$$\mathrm{OLR}_{as} \approx \sigma T_{ct}^4 f + \mathrm{OLR}_{cs}(1-f). \tag{3}$$

This model is similar in some ways to the conceptual model created in (Soden et al., 2008) to examine cross-field correlations between clear-sky and cloud feedbacks.

To get a sense of what the inputs to equation 3 look like, we plot annual- and zonal-mean f, T_{ct}, OLR_{cs}, and OLR_{as} from ERA5 reanalysis in gray in Figure 4. Note the muted latitudinal dependence of OLR_{cs} compared to variations in OLR_{cs} throughout the rest of the globe. This is inconsistent with the notion of radiator fins as significant subtropical maxima in OLR_{cs}, which is why focus on λ_{cs} instead. OLR_{as} does have more significant tropical extrema, but these should not be interpreted as a furnace and radiator fins because the longwave warming effect of deep tropical clouds is balanced by their shortwave cooling effect (Pierrehumbert, 1995; D. L. Hartmann & Berry, 2017).

We test the approximate all-sky radiation from Equation 3 against OLR_{as} directly output from ERA5 analysis, which includes cloud opacities and comprehensive radiative transfer in its calculation. We find that our model does an acceptable job in replicating the reanalysis (Figure 4), which gives us enough confidence in this model to proceed.

We now use Equation 3 to compute the longwave all-sky feedback, λ_{as}. We first assume high cloud temperatures do not change appreciably with warming, consistent with a fixed anvil temperature (FAT) hypothesis (D. Hartmann & Larson, 2002; Zelinka & Hartmann, 2010). Although f can change with warming (Bony et al., 2016; Saint-Lu et al., 2020), the high cloud area feedback is quite uncertain (Wing et al., 2020; Sherwood et al., 2020), so for simplicity we assume f is constant with warming. Differentiating Equation 3 with respect to T_s yields:

$$\lambda_{as} = \lambda_{cs}(1-f). \tag{4}$$

This equation makes it conceptually clear how clouds modify λ_{cs}: the longwave feedback over clouds is 0. Since f is positive definite (Figure 4), $\lambda_{as} \leq \lambda_{cs}$ always. This is well demonstrated in the meridional structure of λ_{as} in Figure 5a. The all-sky feedback looks like a simple translation downward of the clear-sky feedback, and there is still a significant ($\sim$50%) variation in λ_{as} from the subtropics to the deep tropics. Our answer to Question 3 is then: Clouds have a destabilizing influence on the longwave feedback. However, the structure of all-sky feedback looks similar to clear-sky feedback, implying that the RH-dependence from clear-sky effects still dominate the meridional structure.

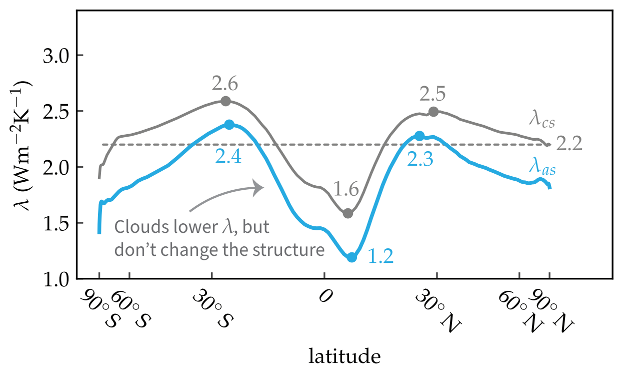

Figure 5. Incorporating clouds into the longwave feedback. Zonal-mean all-sky feedback (λ_{as}, blue) is diagnosed from zonal-mean clear-sky feedback (λ_{cs}, gray) and zonal-mean cloud-top fraction f. See Equation 4 for details. Note the equal-area scaling of the x-axis.

3 Discussion

Our work can be summarized as follows:

1. At high temperatures, variations in RH are sufficient to close the H_2O window, driving deviations in λ_{cs} from the typical value of 2.2 $\mathrm{Wm^{-2}K^{-1}}$ (Figure 1).
2. Furnaces and radiator fins can be interpreted as tropical extrema in zonal-mean λ_{cs} as a consequence of the RH-dependence (Figure 3).
3. Cloud radiative effects can be estimated with a simple equation to reconstruct the all-sky OLR (Figure 4), which we then use to estimate the all-sky feedback. Clouds lower the feedback relative to clear skies, but the RH-dependence of the feedback is still significant (Figure 5).

3.1 Comparison to other work

We have demonstrated a reason for why a large contrast in λ_{cs} emerges in the tropics. However, Zhang et al. (2020) analyzed GCMs and suggested that the dip in zonal mean λ_{cs} to 1 $\mathrm{Wm^{-2}K^{-1}}$ in their study results from local column RH increases. Column RH is fixed in our study and yet we still get a significant tropical dip in λ_{cs} to 1.6 $\mathrm{Wm^{-2}K^{-1}}$. Therefore, this suggests that climatological RH is as important as local RH changes in GCMs in causing tropical deviations from the global mean value of $\lambda_{cs} \approx$ 2.2 $\mathrm{Wm^{-2}K^{-1}}$.

Our results for the zonal-mean feedback cannot be directly compared to other studies of zonal mean feedback (e.g. Feldl and Roe (2013a, 2013b); Armour et al. (2013)) for two reasons. The first is that our λ_{cs} is not equal to the sum of the Planck, Lapse-Rate, and q_v feedbacks, because these feedbacks include "cloud climatological effects" (Yoshimori et al., 2020), i.e. these feedbacks are calculated in the presence of clouds from the control simulation. Furthermore, our λ_{as} is also not equal to this sum of conventional feedbacks, because those feedbacks fix the cloud pressure, whereas we fix the cloud temperature. These issues were discussed in detail by Yoshimori et al. (2020), and our λ_{as} should be comparable to their T-FRAT feedback in which the RH and cloud temperatures are fixed. Further work could explicitly explore such comparisons.

Our new understanding of the state dependence of λ_{cs} gives context to previous results. For example, Meraner et al. (2013); Bloch-Johnson et al. (2021) attributed an increase in equilibrium climate sensitivity to the decrease in λ_{cs} with warming. We expect these variations in λ_{cs} to be enhanced in climates hotter than present-day Earth and conversely to be suppressed in climates cooler than present-day Earth. Our particular calculation of the λ_{cs} phase space assumed that the CO_2 concentration is fixed at 340 ppmv, which neglects the increasingly important role of CO_2 in stabilizing the climate at high CO_2 concentrations (Seeley & Jeevanjee, 2020). However, the strength in our approach of studying the joint dependence of λ_{cs} on T_s and RH is its generality, for our approach can not only be applied to our present-day climate, but to past climates like the Eocene, Pliocene, and Last Glacial Maximum, and to future climates predicted from different RCP scenarios.

Acknowledgments

ERA5 data is available from `https://doi.org/10.24381/cds.bd0915c6`. Data from the PyRADS calculations are available from `https://www.dropbox.com/sh/vam6f6t7vvyj74x/AAAZtYqz-SbaIvvjrzT8l_Wra?dl=0` and will be available in a Zenodo repository upon acceptance. This work was funded by CEMPS at the University of Exeter. We thank Penelope Maher, Stephen Thomson, Hugo Lambert, and Mitchell Koerner for their helpful conversations on this project.

References

Allan, R. P., Shine, K. P., Slingo, A., & Pamment, J. A. (1999). The dependence of clear-sky outgoing long-wave radiation on surface temperature and relative humidity. *Quarterly Journal of the Royal Meteorological Society*, *125*(558), 2103-2126. doi: https://doi.org/10.1002/qj.49712555809

Armour, K. C., Bitz, C. M., & Roe, G. H. (2013). Time-varying climate sensitivity from regional feedbacks. *Journal of Climate*, *26*(13), 4518 - 4534. doi: 10.1175/JCLI-D-12-00544.1

Bloch-Johnson, J., Rugenstein, M., Stolpe, M. B., Rohrschneider, T., Zheng, Y., & Gregory, J. M. (2021). Climate sensitivity increases under higher CO2 levels due to feedback temperature dependence. *Geophysical Research Letters*, *48*(4), e2020GL089074. doi: https://doi.org/10.1029/2020GL089074

Bony, S., Duvel, J., & Le Trent, H. (1995). Observed dependence of the water vapor and clear-sky greenhouse effect on sea surface temperature: comparison with climate warming experiments. *Climate Dynamics*, *11*, 307-320. doi: https://doi.org/10.1007/BF00211682

Bony, S., Stevens, B., Coppin, D., Becker, T., Reed, K. A., Voigt, A., & Medeiros, B. (2016). Thermodynamic control of anvil cloud amount. *Proceedings of the National Academy of Sciences*, *113*(32), 8927–8932. doi: 10.1073/pnas.1601472113

Budyko, M. I. (1969). The effect of solar radiation variations on the climate of the Earth. *Tellus*, *21*(5), 611–619.

Cess, R. (1975). Global climate change: an investigation of atmospheric feedback mechanisms. *Tellus*, *27*(3), 193-198. doi: https://doi.org/10.1111/j.2153-3490.1975.tb01672.x

Cess, R. D., Potter, G. L., Blanchet, J. P., Boer, G. J., Del Genio, A. D., Dqu, M., ... Zhang, M.-H. (1990). Intercomparison and interpretation of climate feedback processes in 19 atmospheric general circulation models. *Journal of Geophysical Research: Atmospheres*, *95*(D10), 16601-16615. doi: https://doi.org/10.1029/JD095iD10p16601

Cess, R. D., Potter, G. L., Blanchet, J. P., Boer, G. J., Ghan, S. J., Kiehl, J. T., ... Yagai, I. (1989). Interpretation of cloud-climate feedback as produced by 14 atmospheric general circulation models. *Science*, *245*(4917), 513–516. doi: 10.1126/science.245.4917.513

Chung, E.-S., Yeomans, D., & Soden, B. J. (2010). An assessment of climate feedback processes using satellite observations of clear-sky olr. *Geophysical Research Letters*, *37*(2). doi: https://doi.org/10.1029/2009GL041889

Dessler, A. E., Yang, P., Lee, J., Solbrig, J., Zhang, Z., & Minschwaner, K. (2008). An analysis of the dependence of clear-sky top-of-atmosphere outgoing longwave radiation on atmospheric temperature and water vapor. *Journal of Geophysical Research: Atmospheres*, *113*(D17). doi: https://doi.org/10.1029/2008JD010137

Feldl, N., & Roe, G. H. (2013a). Four perspectives on climate feedbacks. *Geophysical Research Letters*, *40*(15), 4007-4011. doi: https://doi.org/10.1002/grl.50711

Feldl, N., & Roe, G. H. (2013b). The nonlinear and nonlocal nature of climate feedbacks. *Journal of Climate*, *26*(21), 8289 - 8304. doi: 10.1175/JCLI-D-12-00631.1

Hartmann, D. (2015). *Global physical climatology*. Elsevier Science. Retrieved from `https://books.google.co.uk/books?id=RsScBAAAQBAJ`

Hartmann, D., & Larson, K. (2002). An important constraint on tropical cloud - climate feedback. *Geophysical Research Letters*, *29*(20), 12-1-12-4. doi: https://doi.org/10.1029/2002GL015835

Hartmann, D. L., & Berry, S. E. (2017). The balanced radiative effect of tropical anvil clouds. *Journal of Geophysical Research: Atmospheres*, *122*(9), 5003-5020. doi: https://doi.org/10.1002/2017JD026460

Held, I. M., & Shell, K. M. (2012). Using relative humidity as a state variable in climate feedback analysis. *Journal of Climate*, *25*(8), 2578 - 2582. doi: 10.1175/JCLI-D-11-00721.1

Hersbach, H., Bell, B., Berrisford, P., Hirahara, S., Hornyi, A., Muoz-Sabater, J., … Thpaut, J.-N. (2020). The ERA5 global reanalysis. *Quarterly Journal of the Royal Meteorological Society*, *146*(730), 1999-2049. doi: https://doi.org/10.1002/qj.3803

Jeevanjee, N. (2018). *The physics of climate change: simple models in climate science.* Retrieved from `http://arxiv.org/abs/1802.02695`

Jeevanjee, N., Koll, D. D. B., & Lutsko, N. (2021). Simpsons law and the spectral cancellation of climate feedbacks. *Submitted to Geophysical Research Letters*. doi: https://doi.org/10.1002/essoar.10506744.1

Koll, D. D. B., & Cronin, T. W. (2018). Earth's outgoing longwave radiation linear due to H2O greenhouse effect. *Proceedings of the National Academy of Sciences*, *115*(41), 10293–10298. doi: 10.1073/pnas.1809868115

Koll, D. D. B., & Cronin, T. W. (2019, August). *PyRADS: Python RADiation model for planetary atmosphereS.*

Meraner, K., Mauritsen, T., & Voigt, A. (2013). Robust increase in equilibrium climate sensitivity under global warming. *Geophysical Research Letters*, *40*(22), 5944-5948. doi: https://doi.org/10.1002/2013GL058118

Pierrehumbert, R. T. (1995). Thermostats, radiator fins, and the local runaway greenhouse. *Journal of Atmospheric Sciences*, *52*(10), 1784 - 1806. doi: 10.1175/1520-0469(1995)052⟨1784:TRFATL⟩2.0.CO;2

Raval, A., Oort, A. H., & Ramaswamy, V. (1994). Observed dependence of outgoing longwave radiation on sea surface temperature and moisture. *Journal of Climate*, *7*(5), 807 - 821. doi: 10.1175/1520-0442(1994)007⟨0807:ODOOLR⟩2.0.CO;2

Saint-Lu, M., Bony, S., & Dufresne, J.-L. (2020). Observational evidence for a stability iris effect in the tropics. *Geophysical Research Letters*, *47*(14), e2020GL089059. doi: https://doi.org/10.1029/2020GL089059

Seeley, J. T., & Jeevanjee, N. (2020). H2O windows and CO2 radiator fins: A clear-sky explanation for the peak in equilibrium climate sensitivity. *Geophysical Research Letters*, *48*(4), e2020GL089609. doi: https://doi.org/10.1029/2020GL089609

Sherwood, S. C., Webb, M. J., Annan, J. D., Armour, K. C., Forster, P. M., Hargreaves, J. C., . . . Zelinka, M. D. (2020). An assessment of earth's climate sensitivity using multiple lines of evidence. *Reviews of Geophysics*, *58*(4), e2019RG000678. doi: https://doi.org/10.1029/2019RG000678

Siebesma, A., Bony, S., Jakob, C., & Stevens, B. (2020). *Clouds and climate: Climate science's greatest challenge*. Cambridge University Press. Retrieved from https://books.google.co.uk/books?id=rvXvDwAAQBAJ

Soden, B. J., Held, I. M., Colman, R., Shell, K. M., Kiehl, J. T., & Shields, C. A. (2008). Quantifying climate feedbacks using radiative kernels. *Journal of Climate*, *21*(14), 3504 - 3520. doi: 10.1175/2007JCLI2110.1

Thompson, D. W. J., Bony, S., & Li, Y. (2017). Thermodynamic constraint on the depth of the global tropospheric circulation. *Proceedings of the National Academy of Sciences*, *114*(31), 8181–8186. doi: 10.1073/pnas.1620493114

Wing, A. A., Stauffer, C. L., Becker, T., Reed, K. A., Ahn, M.-S., Arnold, N. P., . . . Zhao, M. (2020). Clouds and convective self-aggregation in a multimodel ensemble of radiative-convective equilibrium simulations. *Journal of Advances in Modeling Earth Systems*, *12*(9), e2020MS002138. doi: https://doi.org/10.1029/2020MS002138

Yoshimori, M., Lambert, F. H., Webb, M. J., & Andrews, T. (2020). Fixed anvil temperature feedback: Positive, zero, or negative? *Journal of Climate*, *33*(7), 2719 - 2739. doi: 10.1175/JCLI-D-19-0108.1

Zelinka, M. D., & Hartmann, D. L. (2010). Why is longwave cloud feedback positive? *Journal of Geophysical Research: Atmospheres*, *115*(D16). doi: https://doi.org/10.1029/2010JD013817

Zelinka, M. D., Myers, T. A., McCoy, D. T., Po-Chedley, S., Caldwell, P. M., Ceppi, P., . . . Taylor, K. E. (2020). Causes of higher climate sensitivity in CMIP6 models. *Geophysical Research Letters*, *47*(1), e2019GL085782. doi: https://doi.org/10.1029/2019GL085782

Zhang, Y., Jeevanjee, N., & Fueglistaler, S. (2020). Linearity of outgoing longwave radiation: From an atmospheric column to global climate models. *Geophysical Research Letters*, *47*(17), e2020GL089235. doi: https://doi.org/10.1029/2020GL089235

Figure 1.

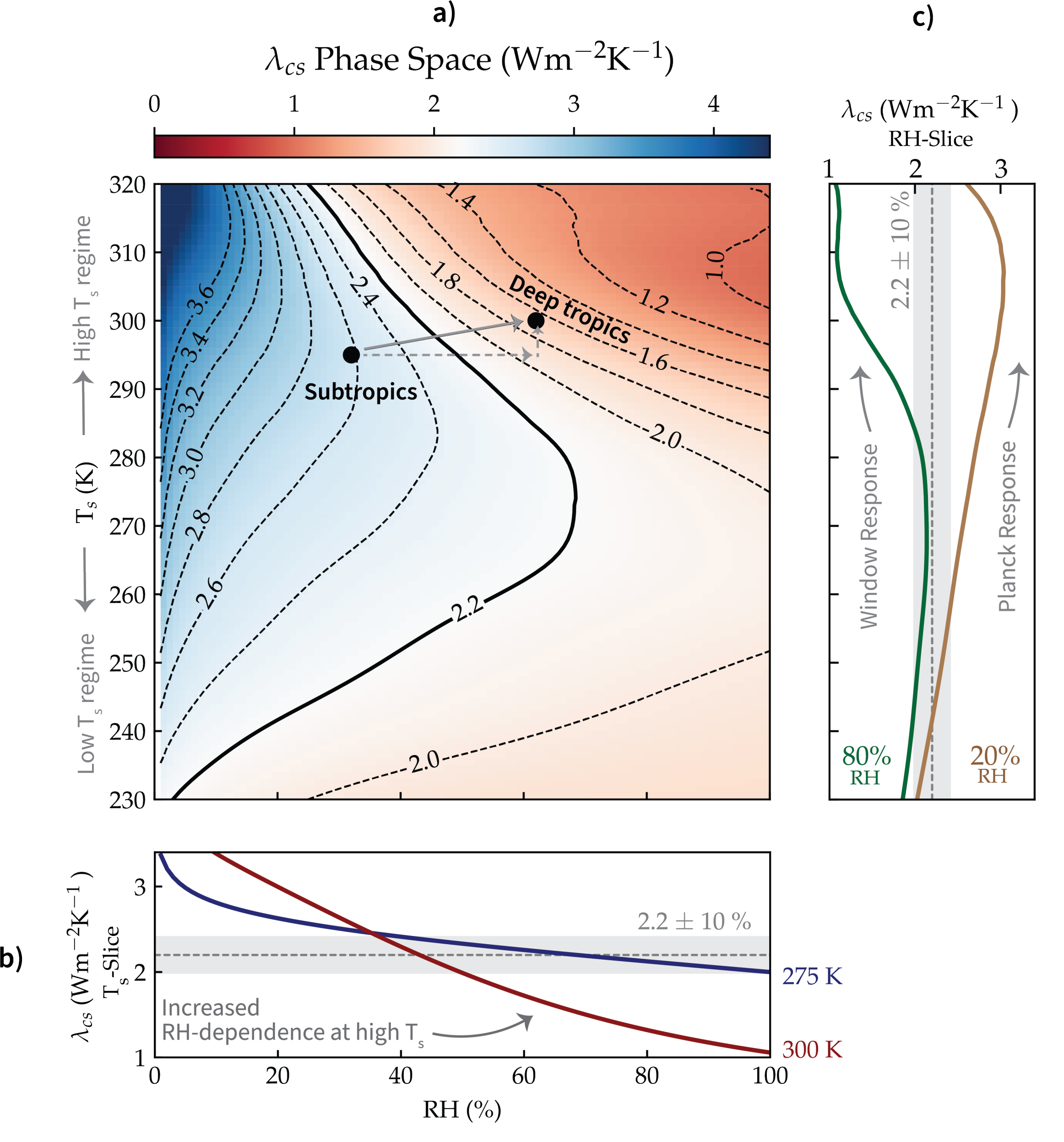

a)
λ_{cs} Phase Space ($Wm^{-2}K^{-1}$)
0
1
2
3
4
1.4
1.0
1.2
1.8
2.4
3.6
3.4
3.2
3.0
2.8
2.6
2.2
2.0
1.6
Deep tropics
Subtropics
High T_s regime
Low T_s regime
T_s (K)
320
310
300
290
280
270
260
250
240
230
c)
λ_{cs} ($Wm^{-2}K^{-1}$)
RH-Slice
2.2 ± 10 %
Window Response
Planck Response
80% RH
20% RH
b)
λ_{cs} ($Wm^{-2}K^{-1}$)
T_s-Slice
Increased RH-dependence at high T_s
275 K
300 K
RH (%)
0
20
40
60
80
100

Figure 2.

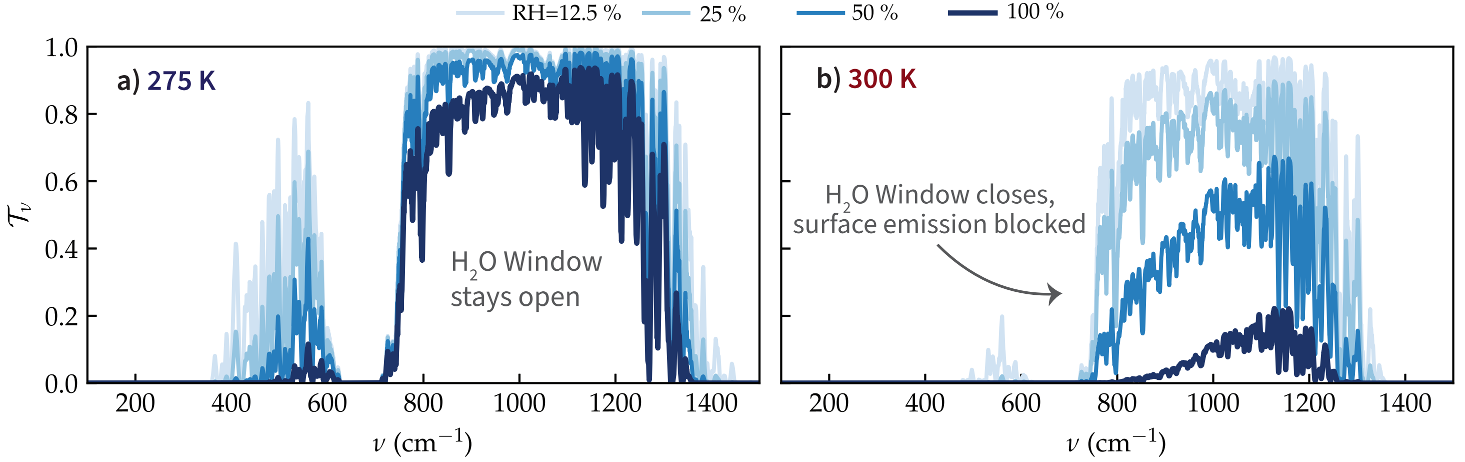
RH=12.5 %
25 %
50 %
100 %
a) 275 K
b) 300 K
$\mathcal{T}_\nu$
H$_2$O Window stays open
H$_2$O Window closes, surface emission blocked
1.0
0.8
0.6
0.4
0.2
0.0
200
400
600
800
1000
1200
1400
ν (cm^{-1})

Figure 3.

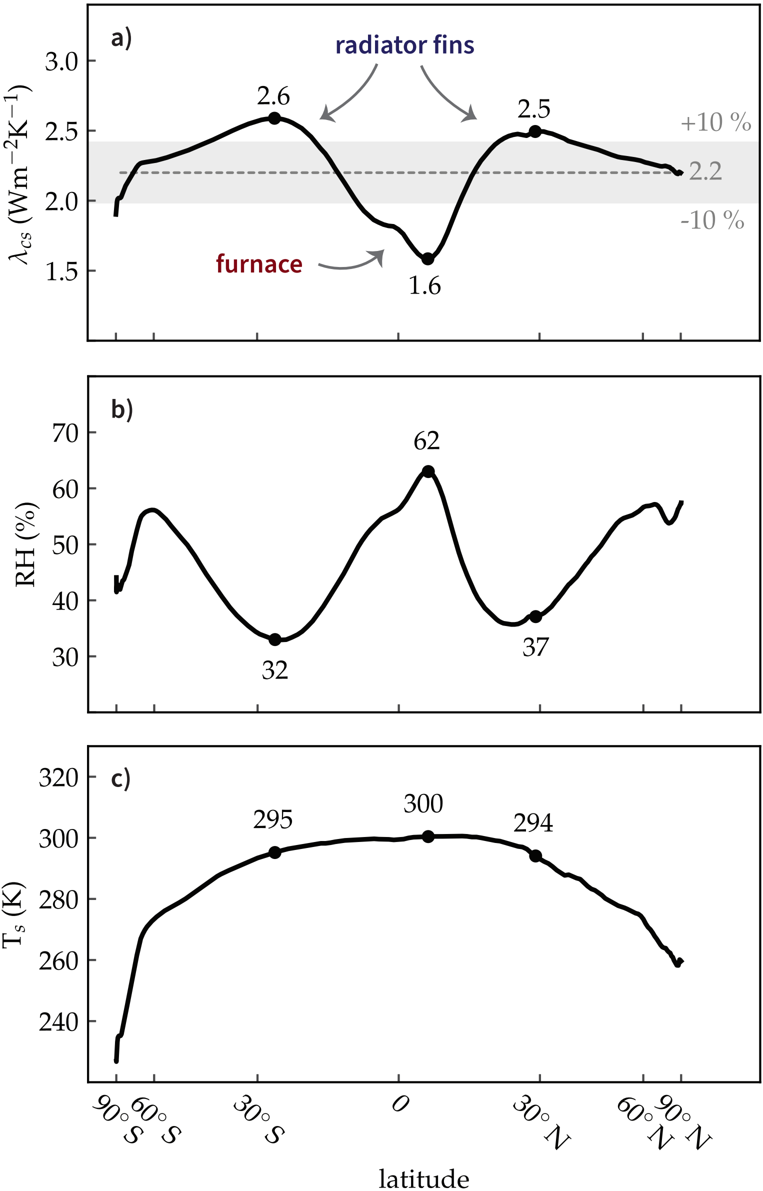
a)
radiator fins
2.6
2.5
+10 %
2.2
-10 %
furnace
1.6
λ_{cs} (Wm^{-2}K^{-1})
3.0
2.5
2.0
1.5
b)
70
60
50
40
30
RH (%)
62
32
37
c)
320
300
280
260
240
T$_s$ (K)
295
300
294
90°S
60°S
30°S
0
30°N
60°N
90°N
latitude

Figure 4.

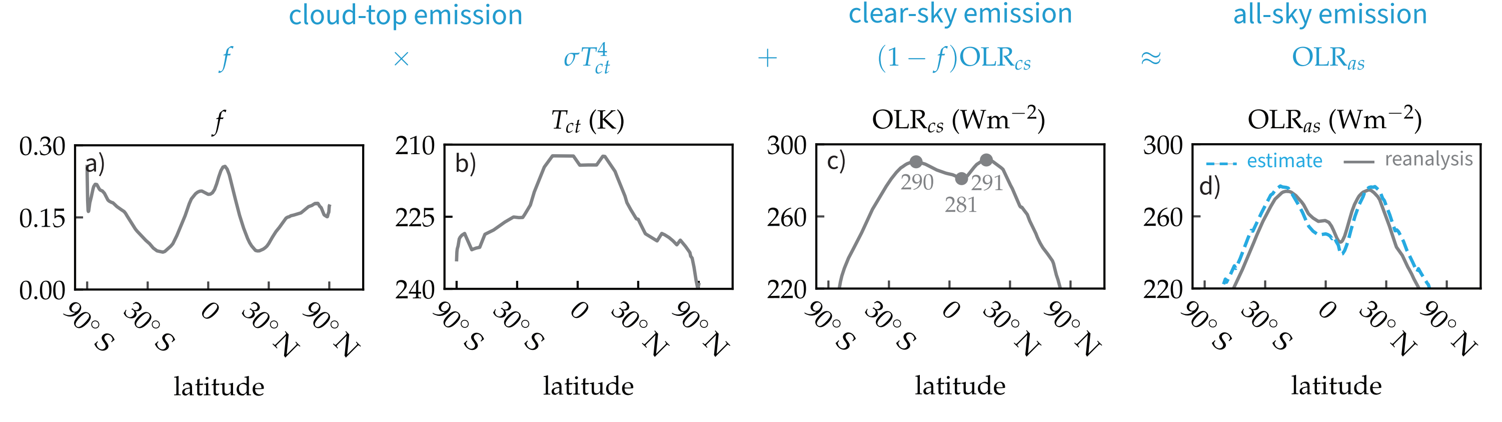
cloud-top emission
clear-sky emission
all-sky emission
$f \times \sigma T_{ct}^4 + (1-f)\mathrm{OLR}_{cs} \approx \mathrm{OLR}_{as}$
f
T_{ct} (K)
OLR_{cs} (Wm^{-2})
OLR_{as} (Wm^{-2})
a)
b)
c)
d)
0.30
0.15
0.00
210
225
240
300
260
220
290
281
291
estimate
reanalysis
90°S
30°S
0
30°N
90°N
latitude

Figure 5.

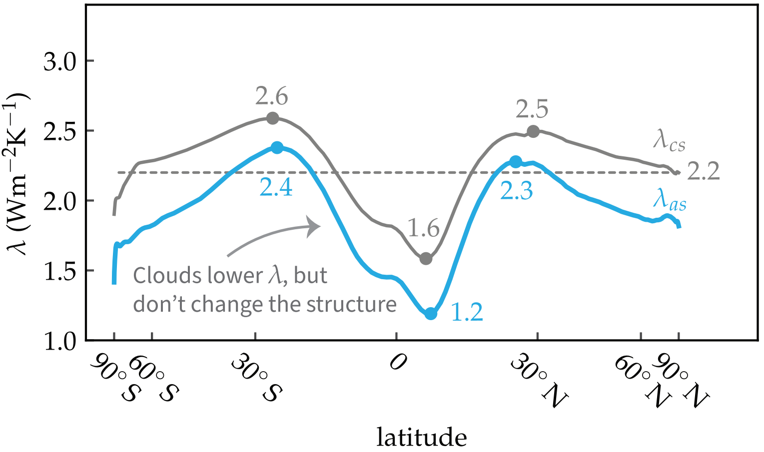

3.0
2.5
2.0
1.5
1.0
λ (Wm⁻²K⁻¹)
2.6
2.5
λ_{cs}
2.2
2.4
2.3
λ_{as}
1.6
1.2
Clouds lower λ, but
don't change the structure
90°S
60°S
30°S
0
30°N
60°N
90°N
latitude